

Space-Time Covariance Matrix Estimation: Loss of Algebraic Multiplicities of Eigenvalues

Faizan A. Khattak, Stephan Weiss, Ian K. Proudler, and John G. McWhirter

Department of Electronic & Electrical Engineering, University of Strathclyde

Glasgow, G1 1XW, Scotland

{faizan.khattak;stephan.weiss;ian.proudler;john.mcwhirter}@strath.ac.uk

Abstract—Parahermitian matrices in almost all cases admit an eigenvalue decomposition (EVD) with analytic eigenvalues. This decomposition is key in order to extend the utility of the EVD from narrowband multichannel signal processing problems to the broadband case, where the EVD factors are frequency dependent. In the frequency domain, the ground truth analytic eigenvalues may intersect, in this paper we discuss why with estimated space-time covariance matrices such algebraic multiplicities are lost, resulting with probability one in analytic, spectrally majorised eigenvalues that no longer intersect. We characterise this phenomenon and some of its profound consequences for broadband multichannel array signal processing.

Index Terms—Space-time covariance, polynomial eigenvalue decomposition, analytic eigenvalue decomposition, estimation.

I. INTRODUCTION

Broadband array processing problems can be conveniently formulated via the space-time covariance matrix $\mathbf{R}[\tau] = \mathcal{E}\{\mathbf{x}[n]\mathbf{x}^H[n-\tau]\} \in \mathbb{C}^{M \times M}$, where the data vector $\mathbf{x}[n] \in \mathbb{C}^M$ holds the signals received by M sensors in discrete time n , $\mathcal{E}\{\cdot\}$ is the expectation operator, and $\{\cdot\}^H$ applies a Hermitian transposition. To solve broadband array problems ranging from multiple-input multiple-output systems [7], [16], [22], broadband beamforming [30], angle of arrival estimation [1], [29], coding [23], [38], subspace detection [19], [20], [31], speech processing [18], and others [32] often requires the diagonalisation of $\mathbf{R}[\tau]$ for all lags τ , also known as strong decorrelation [26], or equivalently the diagonalisation of the cross-spectral density (CSD) matrix $\mathbf{R}(z) = \sum_{\tau} \mathbf{R}[\tau]z^{-\tau}$ [27]. The symmetries of the space-time covariance, $\mathbf{R}[\tau] = \mathbf{R}^H[-\tau]$ mean that $\mathbf{R}(z)$ is a parahermitian matrix, i.e. it is equal to its parahermitian transpose such that $\mathbf{R}^P(z) = \mathbf{R}^H(1/z^*) = \mathbf{R}(z)$.

For the diagonalisation of $\mathbf{R}(z)$, in almost all cases a decomposition $\mathbf{R}(z) = \mathbf{Q}(z)\mathbf{\Lambda}(z)\mathbf{Q}^P(z)$ exists with analytic paraunitary $\mathbf{Q}(z)$ and analytic diagonal and parahermitian $\mathbf{\Lambda}(z)$ [33]. This parahermitian matrix EVD (PhEVD) with its analytic eigenvalues differs from a polynomial EVD (PEVD) [13], which has been shown to converge to a solution where, in the frequency domain, eigenvalues are spectrally majorised [14]. Since the former are non-differentiable, they

require significantly higher approximation orders compared to algorithms that target the PhEVD [36].

In this paper, we will investigate the case where the space-time covariance matrix is estimated from finite data [5], leading to an estimate $\hat{\mathbf{R}}[\tau]$. Any difference between $\mathbf{R}[\tau]$ and $\hat{\mathbf{R}}[\tau]$ results in a perturbation of the eigenvalues and eigenspaces compared to those of $\mathbf{R}[\tau]$. When evaluated at isolated points on the unit circle, $\mathbf{R}(e^{j\Omega_0}) = \mathbf{R}(z)|_{z=e^{j\Omega_0}}$, these perturbations have been linked to the true space-time covariance, the sample size N , and the distance between eigenvalues at Ω_0 [4], [5]. However, the impact of the estimation process on the overall factors of $\hat{\mathbf{R}}(e^{j\Omega})$ for continuous Ω has not been previously investigated and will be the focus of this paper.

Our analysis is organised as follows: we commence with the space-time covariance matrix in Sec. II, for which we define ground truth model that ties the data vector to spatially and temporally uncorrelated source signals via deterministic system components. We also show how the space-time covariance can be estimated from data, and comment on the variance of the estimation error, and its impact on the bin-wise perturbation of the eigenvalues and eigenspaces. The analytic eigenvalue decomposition of the ground truth space-time covariance is outline in Sec. III, while Sec. IV addressed the decomposition of the estimated space-time covariance, and the loss of algebraic multiplicities. Both beneficial and detrimental consequences are outlined in Sec. V, and conclusions are drawn in Sec. VI.

II. SPACE-TIME COVARIANCE MATRIX

A. Source Model

We first derive how the space-time covariance can be formulated based on a model of system components that generate the sensor data $\mathbf{x}[n]$. For this we utilise the model in Fig. 1, where L sources illuminate an M -element measurement vector $\mathbf{x}[n] \in \mathbb{C}^M$. By tying this model to L spatially and temporally uncorrelated zero-mean unit variance signals $s_{\ell}[n]$, $\ell = 1, \dots, L$, the filters $g_{\ell}[n]$ describe the source power spectral densities. The system $\mathbf{H}(z) : \mathbb{C} \rightarrow \mathbb{C}^{M \times L}$ then performs convolutive mixing of these spectrally shaped contributions. Hence for

This work was supported in parts by the Engineering and Physical Sciences Research Council (EPSRC) Grant number EP/S000631/1 and the MOD University Defence Research Collaboration in Signal Processing. Faizan Khattak is the recipient of a Commonwealth Scholarship.

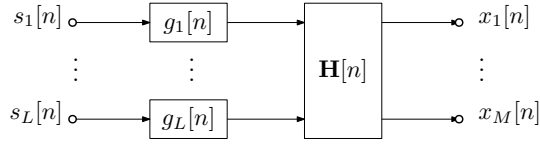


Fig. 1. Source model for space-time covariance matrix.

$\mathbf{R}(z) \bullet \text{---} \circ \mathbf{R}[\tau] = \mathcal{E}\{\mathbf{x}[n]\mathbf{x}^H[n - \tau]\}$, we obtain

$$\mathbf{R}(z) = \mathbf{H}(z) \begin{bmatrix} g_1(z)g_1^P(z) & & \\ & \ddots & \\ & & g_L(z)g_L^P(z) \end{bmatrix} \mathbf{H}^P(z), \quad (1)$$

where $g_\ell(z) \bullet \text{---} \circ g_\ell[n]$.

B. Estimation

In practise, the model in (1) is not available to determine the space-time covariance $\mathbf{R}(z)$. Instead, $\mathbf{R}(z)$ has to be estimated from a finite number of samples, say N , such that $\mathbf{x}[n]$ is only available for $0 \leq n < N$. The entry on the m th row and μ column of $\mathbf{R}[\tau]$ is the cross-correlation between the m th and the μ signal; as an unbiased estimator, [5] suggests to compute

$$\hat{r}_{m\mu}[\tau] = \begin{cases} \frac{1}{N-\tau} \sum_{n=0}^{N-\tau-1} x_m[n+\tau]x_\mu^*[n] & \tau \geq 0; \\ \frac{1}{N+\tau} \sum_{n=0}^{N+\tau-1} x_m[n]x_\mu^*[n-\tau] & \tau < 0. \end{cases} \quad (2)$$

Provided that the source signals $s_\ell[n]$, and therefore the measurements $x_m[n]$, are Gaussian, the variance of this estimate according to [5] is

$$\text{var}\{\hat{r}_{m\mu}[\tau]\} = \frac{1}{(N-|\tau|)^2} \sum_{t=-N+|\tau|+1}^{N-|\tau|-1} (N-|\tau|-|t|) \cdot (r_{mm}[t]r_{\mu\mu}^*[t] - \bar{r}_{m\mu}[\tau+t]\bar{r}_{m\mu}^*[\tau-t]), \quad (3)$$

with $\bar{r}_{m\mu}[\tau] = \mathcal{E}\{x_m[n]x_\mu[n-\tau]\}$ the complementary cross-correlation sequence. Note that due to the bias-free nature of the estimate in (2), the variance in (3) therefore equals the power of the estimation error. It depends on both the sample size, N , as well as the auto- and cross-correlation sequences of the sensor signals.

III. PARAHERMITIAN MATRIX EIGENVALUE DECOMPOSITION

If the data vector $\mathbf{x}[n]$ is generated by a model as in Fig. 1 with stable and causal filters, and is not connected to a multiplexing operation, then $\mathbf{R}(z)$ is analytic in z within a region that contains at the very least the unit circle. Therefore, $\mathbf{R}(z)$ admits a parahermitian matrix or analytic EVD [33], [34],

$$\mathbf{R}(z) = \mathbf{Q}(z)\mathbf{\Lambda}(z)\mathbf{Q}^P(z), \quad (4)$$

where all factors can be analytic. The diagonal matrix $\mathbf{\Lambda}(z) = \text{diag}\{\lambda_1(z), \dots, \lambda_M(z)\}$ contains the M eigenvalues, $\lambda_m(z)$, $m = 1, \dots, M$. The matrix $\mathbf{Q}(z) = [\mathbf{q}_1(z), \dots, \mathbf{q}_M(z)]$

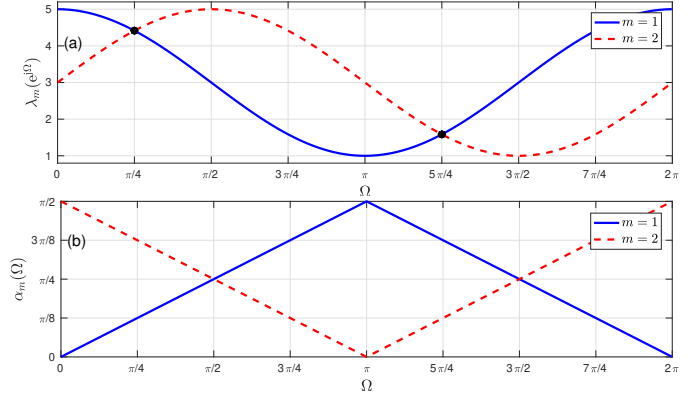


Fig. 2. Example for (a) analytic eigenvalues and (b) Hermitian angles of their corresponding analytic eigenvectors.

holds the corresponding eigenvectors in its columns and is paraunitary, such that $\mathbf{Q}(z)\mathbf{Q}^P(z) = \mathbf{Q}^P(z)\mathbf{Q}(z) = \mathbf{I}$. While the analytic eigenvalues are unique, the eigenvectors can be modified by an arbitrary allpass function [33].

Example 1: Consider the parahermitian matrix

$$\mathbf{R}(z) = \begin{bmatrix} \frac{1-j}{2}z + 3 + \frac{1+j}{2}z^{-1} & \frac{1+j}{2}z^2 + \frac{1-j}{2} \\ \frac{1+j}{2} + \frac{1-j}{2}z^{-2} & \frac{1-j}{2}z + 3 + \frac{1+j}{2}z^{-1} \end{bmatrix} \quad (5)$$

from [33]. This matrix possesses the analytic eigenvalues $\lambda_1(z) = z + 3 + z^{-1}$, and $\lambda_2(z) = jz + 3 - jz^{-1}$, which are shown, evaluated on the unit circle, in Fig. 2(a). The analytic eigenvectors can be selected as $\mathbf{q}_m(z) = [1, \pm z^{-1}]^T / \sqrt{2}$, $m = 1, 2$. The evolution of the eigenvectors along the unit circle is visualised in Fig. 2(b) via the Hermitian angle $\alpha_m(\Omega)$, with $\cos \alpha_m(\Omega) = |\mathbf{q}_1^H(e^{j\Omega})\mathbf{q}_m(e^{j\Omega})|$, whereby the DC value for the first eigenvalue, $\mathbf{q}_1^H(e^{j0})$, is chosen as an arbitrary reference point. This angle is insensitive to the ambiguity of the eigenvectors with respect to arbitrary allpass functions. Note that due to analyticity, both eigenvalues and the angles of the eigenvectors evolve smoothly. \triangle

IV. EIGENVALUES OF AN ESTIMATED SPACE-TIME COVARIANCE MATRIX

A. Eigenvalues at an Algebraic Multiplicity

Because in practice, $\mathbf{R}[\tau]$ needs to be estimated from N snapshots of data, $\mathbf{x}[n]$, $n = 0, \dots, (N-1)$, we generally will perform an EVD factorisation of $\hat{\mathbf{R}}[\tau]$ rather than of $\mathbf{R}[\tau]$. As outlined in Sec. II-B, the variance of the unbiased estimator depends on both the ground truth $\mathbf{R}[\tau]$ and the sample size N . Thus, the eigenvalues of $\hat{\mathbf{R}}[\tau]$ are perturbed, and now are random variables [4]; this is well-known from random matrix theory, see e.g. [8], [15], [21].

This is particularly noticeable where the eigenvalues of $\mathbf{R}(z)$ possess an algebraic multiplicity greater than one, i.e. where at least two eigenvalues are identical. When now inspecting the eigenvalues of $\hat{\mathbf{R}}(z)$ instead, we find that these eigenvalues are drawn from probability distributions, and that we thus obtain distinct eigenvalues with probability one, unless for the sample size we have $N \rightarrow \infty$.

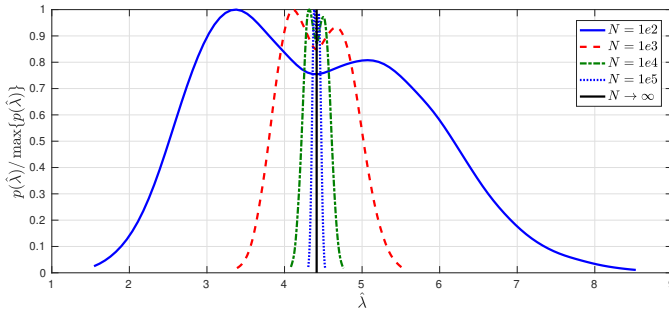


Fig. 3. Normalised approximate probability density functions $p(\hat{\lambda})$ for eigenvalues $\hat{\lambda}$ of $\hat{\mathbf{R}}(e^{j\pi/4})$, estimated for a number of different sample sizes N , from each 10^5 instances.

Example 2: Based on Example 1, we utilise the source model in Fig. 1 with $\mathbf{H}(z) = \mathbf{Q}(z)$, and $g_m(z) = \sqrt{\lambda_m(z)}$, $m = 1, 2$ to generate an ensemble of 10^5 data sequences with various sample sizes N , from which the distribution of the eigenvalues $\hat{\lambda}_m(e^{j\Omega})$ of $\hat{\mathbf{R}}(e^{j\Omega})$ at $\Omega = \frac{\pi}{4}$ is estimated. Note from Fig. 2(a) that for $\Omega = \frac{\pi}{4}$, the ground truth eigenvalues $\lambda_1(e^{j\pi/4}) = \lambda_2(e^{j\pi/4}) = 3 + \sqrt{2} \approx 4.41$. The approximated distribution of the eigenvalues of $\hat{\mathbf{R}}(e^{j\pi/4})$ is shown in Fig. 3; note that only for the transition $N \rightarrow \infty$ will we obtain two identical eigenvalues, i.e. an algebraic multiplicity of two. \triangle

B. Impact on Analytic Eigenvalues

Sec. IV-A has argued how at a given frequency Ω_0 with an algebraic multiplicity of the eigenvalues of $\mathbf{R}(e^{j\Omega_0})$ greater than one, the eigenvalues $\hat{\lambda}$ of $\hat{\mathbf{R}}(e^{j\Omega_0})$ must be distinct with probability one. Since the eigenvalues $\lambda(e^{j\Omega})$ are random variable for all Ω , $\hat{\mathbf{R}}(e^{j\Omega})$ has distinct eigenvalues with probability one for all frequencies Ω .

Since $\hat{\mathbf{R}}(z)$ is analytic, e.g. because it is estimated with only finite support $|\tau| \leq \tau_{\max}$, its eigenvalues $\hat{\lambda}_m(z)$, $m = 1, \dots, M$ must also be analytic. However, since the eigenvalues are distinct at all frequencies, if ordered in descending values, they must now be strictly spectrally majorised, such that on the unit circle

$$\hat{\lambda}_m(e^{j\Omega}) > \hat{\lambda}_{m+1}(e^{j\Omega}) \quad \forall \Omega, m = 1, \dots, (M-1). \quad (6)$$

Spectral majorisation has been a feature of two families of polynomial EVD algorithms [13], [14], [23]–[25], but here it is not an algorithmic detail but expresses the nature of the estimated space-time covariance matrix.

C. Impact of Sample Size

It is interesting to note that the loss of algebraic multiplicities or the strict spectral majorisation of eigenvalues cannot be alleviated by enhancing estimates. This includes, for example, limiting the perturbation of eigenvalues through optimum support estimation [6], [10]. Bypassing some estimation errors through performing a system identification of the source model [11] generally still retains some finite error, for example due to observation noise. Simply increasing the sample size N on which the estimate is based will also bypass this challenge unless the transition $N \rightarrow \infty$ is made [5].

A detrimental effect occurs for the analytic EVD as N increases. Let $\lambda'_m(e^{j\Omega})$ and $\mathbf{q}'_m(e^{j\Omega})$ be permuted versions of the EVD factors $\lambda_m(e^{j\Omega})$ and $\mathbf{q}_m(e^{j\Omega})$ of $\mathbf{R}(e^{j\Omega})$, such that the modified eigenvalues $\lambda'_m(e^{j\Omega})$ are spectrally majorised,

$$\lambda'_m(e^{j\Omega}) \geq \lambda'_{m+1}(e^{j\Omega}) \quad \forall \Omega, m = 1, \dots, (M-1). \quad (7)$$

If the analytic eigenvalues $\lambda_m(e^{j\Omega})$ are not spectrally majorised, then $\lambda'_m(e^{j\Omega})$ will only piece-wise analytic: at frequencies where permutations occur, they will be continuous but not infinitely differentiable. Further the corresponding eigenvectors $\mathbf{q}'_m(e^{j\Omega})$ will be discontinuous at permutation frequencies [33]. Thus, as N increases, we find that

$$\hat{\lambda}_m(e^{j\Omega}) \longrightarrow \lambda'_m(e^{j\Omega}). \quad (8)$$

Therefore, with increasing sample size N , $\hat{\lambda}_m(e^{j\Omega})$ tends towards a function that is not infinitely differentiable. Worse, the eigenvectors of $\hat{\mathbf{R}}(z)$, $\hat{\mathbf{q}}_m(e^{j\Omega})$, converge towards non-differentiable functions, even though they do not reach these for finite N . Thus, while with increasing N both eigenvalues and eigenvectors remain analytic, they become more and more difficult to approximate by polynomials or Laurent polynomials [33], requiring them to be of higher orders than for a lower value of N .

Example 3: Taking the setup of Example 2, we inspect the analytic eigenvalues $\hat{\lambda}_m(e^{j\Omega})$ and eigenvectors $\hat{\mathbf{q}}_m(e^{j\Omega})$ across the range $\Omega = (0; 2\pi)$. These are extracted by taking sufficiently long discrete Fourier transforms (DFTs) of $\hat{\mathbf{R}}[\tau]$, and performing an EVD in each DFT bin. Due to (6), it is straightforward to associate the eigenvalues across the DFT bins [36]. The eigenvectors in individual frequency bins will not be phase-aligned; this however does not affect the subspaces in which these analytic eigenvectors exist [35], and the Hermitian angle evaluated in Example 1 will measure the smoothness of these subspaces.

Fig. 4 shows the case of a sample size $N = 10^2$. Due to this small size, the estimation error can be significant, particularly if the support of $\mathbf{R}[\tau]$ is overestimated [5]. Here and in the following examples, the support is optimised to yield the smallest possible estimation error [6]. Nonetheless, the eigenvalues and eigenspaces are perturbed and significantly deviate from the eigenvalues and eigenvector angles of the ground truth space-time covariance $\mathbf{R}[\tau]$.

For $N = 10^4$ in Fig. 5, the eigenvalues $\hat{\lambda}_m(e^{j\Omega})$ are strictly spectrally majorised according to (6) and now follow $\lambda_m(e^{j\Omega})$ closely on a bin-wise basis. However, permutations w.r.t. $\lambda_m(e^{j\Omega})$ occur at $\Omega = \frac{\pi}{4}$ and $\Omega = \frac{5\pi}{4}$. The angles $\alpha_m(\Omega)$ of the associated eigenvectors $\hat{\mathbf{q}}(e^{j\Omega})$ closely follow those of $\mathbf{q}_m(e^{j\Omega})$ on a bin-wise basis, but are also permuted at $\Omega = \frac{\pi}{4}$ and $\Omega = \frac{5\pi}{4}$. Since $\mathbf{q}'_m(e^{j\Omega})$ would be discontinuous at those points, but $\hat{\mathbf{q}}(e^{j\Omega})$ has to be analytic, some sharp transitions occur around the permutation frequencies.

The results for a further increase to $N = 10^6$ are shown in Fig. 6. The approximation of a discontinuity of the Hermitian angles $\alpha_m(e^{j\Omega})$ in Fig. 6(b) indicates that the eigenvalues $\hat{\lambda}_m(e^{j\Omega})$ in Fig. 6(a) remain strictly spectrally majorised.

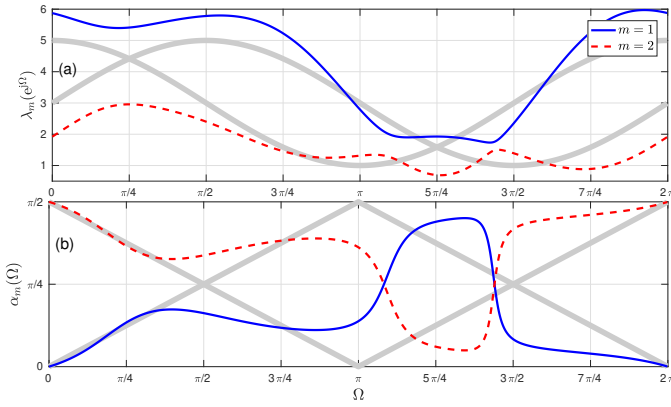


Fig. 4. (a) eigenvalues $\hat{\lambda}_m(e^{j\Omega})$ for $N = 100$ (coloured curves) and ground truth $\lambda_m(e^{j\Omega})$ (in grey, underlaid); Hermitian angles $\alpha_m(\Omega)$ for the corresponding eigenvectors $\hat{\mathbf{q}}(e^{j\Omega})$ and $\mathbf{q}(e^{j\Omega})$.

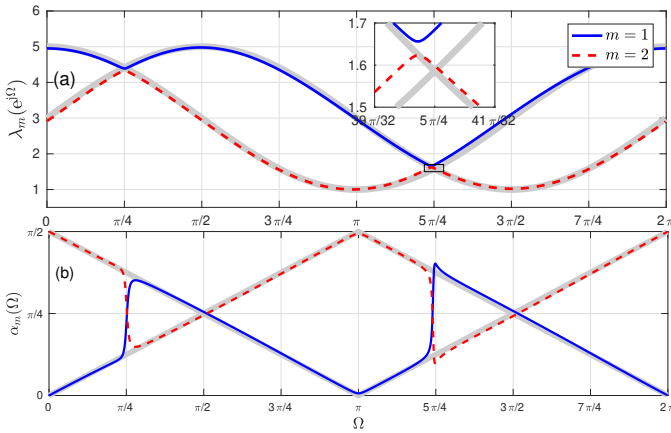


Fig. 5. (a) eigenvalues $\hat{\lambda}_m(e^{j\Omega})$ for $N = 10^4$ (coloured curves) and ground truth $\lambda_m(e^{j\Omega})$ (in grey, underlaid); Hermitian angles $\alpha_m(\Omega)$ for the corresponding eigenvectors $\hat{\mathbf{q}}(e^{j\Omega})$ and $\mathbf{q}(e^{j\Omega})$.

Compared to Fig. 5(b), the transition at the permutation frequencies $\Omega = \frac{\pi}{4}$ and $\Omega = \frac{5\pi}{4}$ is now sharpened, and show behaviour similar to Gibbs phenomena when approximating discontinuities. As a consequence, the eigenvalues $\hat{\mathbf{q}}_m(z)$ need a high approximation order or than those obtainable for a smaller sample size N . \triangle

V. IMPACT ON APPLICATIONS

The strict spectral majorisation of eigenvalues of an estimated space-time covariance matrix can have both positive and negative consequences, which this section briefly highlights.

A. Subspace Methods

For subspace-based methods such as the polynomial multiple signal classification (P-MUSIC) approach [1], [9], [29] or transient signal detection in the noise-only subspace [19], [20], [31], an accurate estimation of the signal-plus-noise and noise-only subspaces is required. The effect caused by permutations of the ground truth analytic EVD factors causes an increase in the approximation orders for the eigenvectors, and hence for

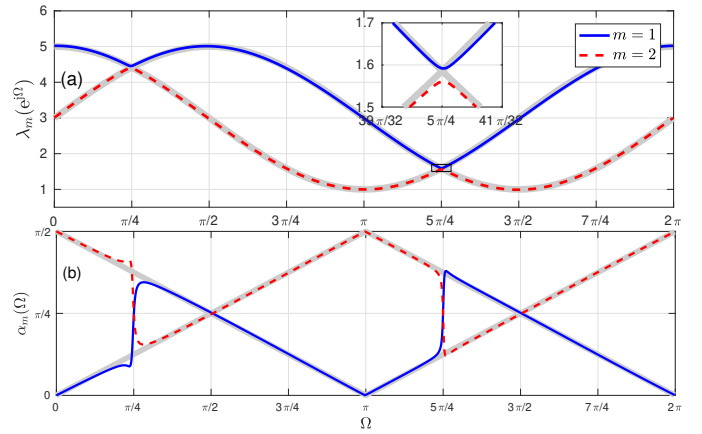


Fig. 6. (a) eigenvalues $\hat{\lambda}_m(e^{j\Omega})$ for $N = 10^6$ (coloured curves) and ground truth $\lambda_m(e^{j\Omega})$ (in grey, underlaid); Hermitian angles $\alpha_m(\Omega)$ for the corresponding eigenvectors $\hat{\mathbf{q}}(e^{j\Omega})$ and $\mathbf{q}(e^{j\Omega})$.

computational complexity that the paraunitary matrices incur when implemented.

Additionally, since the permutations at algebraic multiplicities greater than one of the eigenvalues of $\hat{\mathbf{R}}(z)$ cause switching between subspaces in $\hat{\mathbf{R}}(z)$, the switching itself and the associated Gibbs-type phenomena that could be observed in Example 3 — see Fig. 6(b) — may cause challenges when performing projections.

B. Spectral Majorisation

Applications such as subband coding are optimal in terms of the coding gain if the space-time covariance matrix of the subband signals is strongly decorrelated, i.e. if $\mathbf{R}[\tau]$ is diagonalised, and if its eigenvalues are spectrally majorised [26]. Methods such as in [23], [25] and signal compaction approaches [17] rely on this, and are supported by a number of numerical techniques to calculate the decomposition in (4). This includes the class of second order sequential best rotation (SBR2) and sequential matrix diagonalisation (SMD) algorithms and their variants [2], [13], [23]–[25], [28], which tend — or in some cases are guaranteed [14] — to converge to the spectrally majorised solution. This is a requirement for maximising the coding gain.

C. Analytic EVD of Multiplexed Systems

If the data vector $\mathbf{x}[n]$ emerges from a multiplexing operation, such as for subband coding [23], then the analytic EVD of the ground truth space-time covariance $\mathbf{R}(z)$ does not exist [34]. This is due to the eigenvalues possessing a longer periodicity of $2\pi F$, with F representing the multiplexing factor. However, spectral majorisation will enforce a 2π periodicity, such that an analytic EVD becomes feasible. This has been noted in [34] but without realising that the estimation error when estimating the space-time covariance from finite data, and the associated loss of algebraic multiplicities greater than one, is responsible for this beneficial effect.

VI. CONCLUSIONS

In this paper, we have investigated a fundamental effect that results in the loss of algebraic multiplicities greater than one in the eigenvalues of a space-time covariance matrix that is estimated from finite data. This effect cannot be alleviated by increasing the sample size; rather, such an increase will result in the analytic EVD factors requiring an increasing order if the ground-truth eigenvalues intersect, as non-differentiabilities and discontinuities have to be approximated when extracting the eigenvalues and eigenvectors of such an estimated space-time covariance matrix.

In terms of applications, the effect can be both beneficial or detrimental, and favours a revival of algorithms that target spectrally majorised eigenvalues for polynomial matrix factorisations, which are supported by substantial algorithmic developments and implementations [3], [12]. Alternatively, analytic eigenvalue and eigenvector extraction algorithms [35]–[37], [39] can also yield such solutions with guaranteed spectral majorisation where current time domain methods may fail due to a large dynamic range in the eigenvalues.

REFERENCES

- [1] M. Alrmah, S. Weiss, and S. Lambotharan. An extension of the MUSIC algorithm to broadband scenarios using polynomial eigenvalue decomposition. In *EUSIPCO*, pp. 629–633, Barcelona, Spain, Aug. 2011.
- [2] J. Corr, K. Thompson, S. Weiss, J. McWhirter, S. Redif, and I. Proudler. Multiple shift maximum element sequential matrix diagonalisation for parahermitian matrices. In *IEEE SSP*, pages 312–315, Gold Coast, Australia, June 2014.
- [3] F. K. Coutts, I. K. Proudler, and S. Weiss. Efficient implementation of iterative polynomial matrix evd algorithms exploiting structural redundancy and parallelisation. *IEEE Trans. CAS I: Regular Papers*, 66(12):4753–4766, Dec. 2019.
- [4] C. Delaosa, F. K. Coutts, J. Pestana, and S. Weiss. Impact of space-time covariance estimation errors on a parahermitian matrix EVD. In *10th IEEE SAM*, pages 1–5, July 2018.
- [5] C. Delaosa, J. Pestana, N. J. Goddard, S. Somasundaram, and S. Weiss. Sample space-time covariance matrix estimation. In *IEEE ICASSP*, pp. 8033–8037, May 2019.
- [6] C. Delaosa, J. Pestana, N. J. Goddard, S. D. Somasundaram, and S. Weiss. Support estimation of a sample space-time covariance matrix. In *SSPD*, Brighton, UK, May 2019.
- [7] J. Foster, J. McWhirter, S. Lambotharan, I. Proudler, M. Davies, and J. Chambers. Polynomial matrix QR decomposition for the decoding of frequency selective multiple-input multiple-output communication channels. *IET Signal Proc.*, 6(7):704–712, Sep. 2012.
- [8] M. Greco, S. Fortunati, and F. Gini. Maximum likelihood covariance matrix estimation for complex elliptically symmetric distributions under mismatched conditions. *Signal Proc.*, 104:381–386, 2014.
- [9] A. Hogg, V. Neo, S. Weiss, C. Evers, and P. Naylor. A polynomial eigenvalue decomposition music approach for broadband sound source localization. In *WASPAA*, New Paltz, NY, Oct. 2021.
- [10] F. Khattak, I. K. Proudler, and S. Weiss. Support estimation of analytic eigenvectors of parahermitian matrices. In *Int. Conf. on Recent Advances in Electrical Eng. & Computer Sciences*, Islamabad, Pakistan, Oct. 2022.
- [11] F. A. Khattak, I. K. Proudler, and S. Weiss. Enhanced space-time covariance estimation based on a system identification approach. In *SSPD*, London, UK, Sep. 2022.
- [12] F. A. Khattak, S. Weiss, and I. K. Proudler. Fast givens rotation approach to second order sequential best rotation algorithms. In *SSPD*, pp. 40–44, Edinburgh, Scotland, Sep. 2021.
- [13] J. G. McWhirter, P. D. Baxter, T. Cooper, S. Redif, and J. Foster. An EVD Algorithm for Para-Hermitian Polynomial Matrices. *IEEE Trans. SP*, 55(5):2158–2169, May 2007.
- [14] J. G. McWhirter and Z. Wang. A novel insight to the SBR2 algorithm for diagonalising para-hermitian matrices. In *11th IMA Conf. Math. in Sig. Proc.*, Birmingham, UK, December 2016.
- [15] X. Mestre. On the asymptotic behavior of the sample estimates of eigenvalues and eigenvectors of covariance matrices. *IEEE Trans. SP*, 56(11):5353–5368, Nov 2008.
- [16] X. Mestre and D. Gregoratti. A parallel processing approach to filterbank multicarrier MIMO transmission under strong frequency selectivity. In *IEEE ICASSP*, pp. 8078–8082, May 2014.
- [17] V. Neo, C. Evers, S. Weiss, and P. A. Naylor. Polynomial matrix eigenvalue decomposition exploiting spherical microphone array processing. *IEEE Trans. ASLP*, submitted 2022.
- [18] V. W. Neo, C. Evers, and P. A. Naylor. Polynomial matrix eigenvalue decomposition of spherical harmonics for speech enhancement. In *IEEE ICASSP*, pages 786–790, May 2021.
- [19] V. W. Neo, S. Weiss, S. W. McKnight, A. O. T. Hogg, and P. A. Naylor. Polynomial eigenvalue decomposition-based target speaker voice activity detection in the presence of competing talkers. In *IWAENC*, Bamberg, Germany, Sep. 2022.
- [20] V. W. Neo, S. Weiss, and P. A. Naylor. A polynomial subspace projection approach for the detection of weak voice activity. In *SSPD*, pp. 1–5, London, UK, Sept. 2022.
- [21] E. Oilila, D. E. Tyler, V. Koivunen, and H. V. Poor. Complex elliptically symmetric distributions: Survey, new results and applications. *IEEE Trans. SP*, 60(11):5597–5625, 2012.
- [22] A. I. Pérez-Neira, M. Caus, R. Zakaria, D. L. Ruyet, E. Kofidis, M. Haardt, X. Mestre, and Y. Cheng. MIMO signal processing in offset-QAM based filter bank multicarrier systems. *IEEE Trans. SP*, 64(21):5733–5762, November 2016.
- [23] S. Redif, J. McWhirter, and S. Weiss. Design of FIR paraunitary filter banks for subband coding using a polynomial eigenvalue decomposition. *IEEE Trans. SP*, 59(11):5253–5264, November 2011.
- [24] S. Redif, S. Weiss, and J. McWhirter. Sequential matrix diagonalization algorithms for polynomial EVD of parahermitian matrices. *IEEE Trans. SP*, 63(1):81–89, Jan. 2015.
- [25] S. Redif, S. Weiss, and J. G. McWhirter. An approximate polynomial matrix eigenvalue decomposition algorithm for para-hermitian matrices. In *IEEE ISSPIT*, pp. 421–425, Bilbao, Spain, Dec. 2011.
- [26] P. Vaidyanathan. Theory of optimal orthonormal subband coders. *IEEE Trans. SP*, 46(6):1528–1543, June 1998.
- [27] P. P. Vaidyanathan. *Multirate Systems and Filter Banks*. Prentice Hall, Englewood Cliffs, 1993.
- [28] Z. Wang, J. G. McWhirter, J. Corr, and S. Weiss. Multiple shift second order sequential best rotation algorithm for polynomial matrix EVD. In *EUSIPCO*, pp. 844–848, Nice, France, Sep. 2015.
- [29] S. Weiss, M. Alrmah, S. Lambotharan, J. McWhirter, and M. Kaveh. Broadband angle of arrival estimation methods in a polynomial matrix decomposition framework. In *IEEE CAMSAP*, pp. 109–112, St. Martin, French Antilles, Dec. 2013.
- [30] S. Weiss, S. Bendoukha, A. Alzin, F. Coutts, I. Proudler, and J. Chambers. MVDR broadband beamforming using polynomial matrix techniques. In *EUSIPCO*, pp. 839–843, Nice, France, Sep. 2015.
- [31] S. Weiss, C. Delaosa, J. Matthews, I. Proudler, and B. Jackson. Detection of weak transient signals using a broadband subspace approach. In *SSPD*, pp. 65–69, Edinburgh, Scotland, Sep. 2021.
- [32] S. Weiss, N. J. Goddard, S. Somasundaram, I. K. Proudler, and P. A. Naylor. Identification of broadband source-array responses from sensor second order statistics. In *SSPD*, pp. 1–5, London, UK, Dec. 2017.
- [33] S. Weiss, J. Pestana, and I. K. Proudler. On the existence and uniqueness of the eigenvalue decomposition of a parahermitian matrix. *IEEE Trans. SP*, 66(10):2659–2672, May 2018.
- [34] S. Weiss, J. Pestana, I. K. Proudler, and F. K. Coutts. Corrections to “On the existence and uniqueness of the eigenvalue decomposition of a parahermitian matrix”. *IEEE Trans. SP*, 66(23):6325–6327, Dec. 2018.
- [35] S. Weiss, I. Proudler, F. Coutts, and F. Khattak. Eigenvalue decomposition of a parahermitian matrix: Extraction of analytic eigenvectors. *IEEE Trans. SP*, submitted 2022.
- [36] S. Weiss, I. K. Proudler, and F. K. Coutts. Eigenvalue decomposition of a parahermitian matrix: Extraction of analytic eigenvalues. *IEEE Trans. SP*, 69:722–737, Jan. 2021.
- [37] S. Weiss, I. K. Proudler, F. K. Coutts, and J. Pestana. Iterative approximation of analytic eigenvalues of a parahermitian matrix EVD. In *IEEE ICASSP*, Brighton, UK, May 2019.
- [38] S. Weiss, S. Redif, T. Cooper, C. Liu, P. Baxter, and J. McWhirter. Paraunitary oversampled filter bank design for channel coding. *EURASIP J. Advances Sig. Proc.*, 2006:1–10, 2006.
- [39] S. Weiss, J. Selva, and M. D. Macleod. Measuring smoothness of trigonometric interpolation through incomplete sample points. In *28th EUSIPCO*, pp. 2319–2323, Amsterdam, Netherlands, Jan. 2021.